Postprint of: Gordziej-Zagórowska M., Urbańska-Galewska E., Deniziak P., Experimental investigation of joint with positive eccentricity in CFS truss, Thin-Walled Structures, Vol. 157 (2020), 106998, DOI: 10.1016/j.tws.2020.106998

Experimental investigation of joint with positive eccentricity in CFS truss

Małgorzata Gordziej-Zagórowska [a], Elżbieta Urbańska-Galewska [a], Patryk Deniziak [a]
[a] *Department of Civil and Environmental Engineering, Gdańsk University of Technology, Poland*

Keywords:
stability, truss, eccentricities in the truss joints, experimental tests

Abstract

Due to technological restrictions, in the case of trusses made of CFS open cross-sections, positive eccentricities in the truss joints have become very frequent. Therefore studies concerning the load-bearing capacity of truss joints with positive eccentricity were undertaken. It was assumed that the resistance of cold-formed steel (CFS) open cross-section truss joints located on compression chords and with positive eccentricity is greater than that which results from hitherto known methods of steel structure dimensioning. In order to confirm the hypothesis, experimental studies were conducted. A series of 5 full-scale research models was subjected to destructive tests to determine the deformation forms and strains of the hat-section walls in the area of the eccentric joint. Forms of truss chord stability loss under compression and bending were identified.The course of research and analysis of results were described in the article. Than comparative analysis of the outcomes of the experimental tests and the results of analytical calculations carried out according to Eurocode standards was done, and the obtained results confirmed the usefulness of the undertaken research. The obtained results did not allow for explicit confirmation of the research hypothesis at this stage, but constituted the basis for validation of the numerical model which has been elaborated. Currently, the authors carry out a variety of numerical analysis.

1. Introduction

Cold-formed steel (CFS) members are used more and more commonly in industrial buildings, not only as secondary framing members but also as main bearing elements such

as roof trusses and columns. As a result, new research problems appear. Both individual structural elements such as beams and columns [1–4] and entire parts of the structure, including lattice girders, are subjected to testing [5–7].

Modern lightweight technology used in the production of steel trusses affects their shape, particularly the construction of joints and, as a result, eccentricities frequently appear in the trusses' joints. This can induce additional local bending and shearing forces in the truss chords [8]. In the case of lattice structures composed of circular, square or rectangular hollow sections, the eccentricity influence on the static design resistances of the welded joints has been precisely investigated [9,10]. Detailed information about such joints can be found, among others in publications [9], [11], [12], [13] and in the standard [14]. The information included in these works shows that the load carrying capacity of joints with positive eccentricities is lower than that of joints without eccentricities (e=0). On the other hand, in joints with negative eccentricities the opposite is true; their load carrying capacity is higher.

However, in the case of trusses made of CFS open cross-sections, diagonals are attached to chords by bolts. Trusses' chords are most often designed with hat-sections or members made of two channels, and diagonals are usually made of single channel sections. The use of the above mentioned open cross-sections affects the way joints are shaped. Diagonals are inserted into the cross-sections of the chords, as was done in [6,15], or as presented in Figure 1. The proper arrangement of mechanical connectors in the truss joints causes that brace members must be shifted outside, as shown in Figure 1. This results in the creation of positive eccentricities in the truss joints, and hence bending moments and shear forces in the chords of lattice girders. Those additional internal forces should be taken into account when truss members are designed.

In engineering practice, the dimensioning of truss chords made of CFS members taking into account positive eccentrics, in accordance with current European standards [14,16–18], is performed using a simplified method. However, taking into account the additional bending and shear between the points of intersection of the diagonals' axes

causes an increase in the strain of the bottom chord cross-section in the area of the joint. As a result, the cross-section of the chord should be increased along its entire length or, as presented in the work [19], strengthening cover plates should be made in the nodal zone (Fig.2).

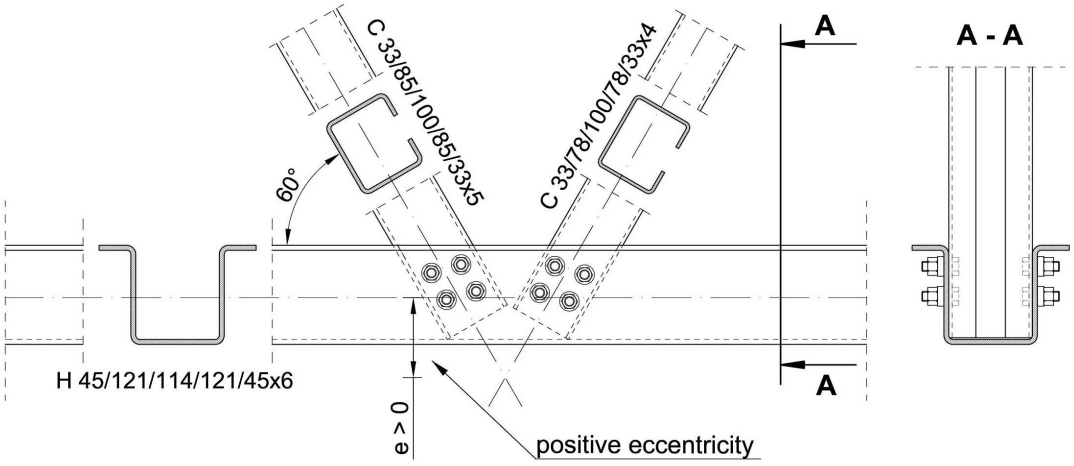

Fig.1. Positive eccentricity in the bolted truss joint made from CFS open cross-sections.

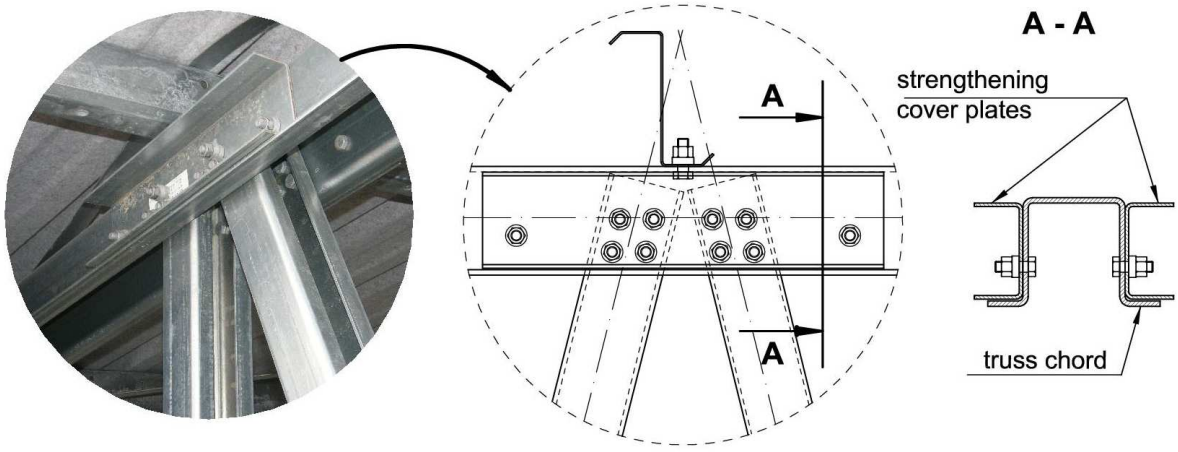

Fig.2. Joint with strengthening cover plates [8].

2. State of the art

Most of the studies of CFS members undertaken so far have been carried out on single compressed [20–23] or bent structural elements [3,24–28]. The issue of wall stability under the influence of shear and bending was investigated by Pham and Hancock [29,30], and the results of experimental studies were used to validate the FEM model. Crisan,

Ungureanu, and Dubina, in turn, conducted full-scale stability tests of both perforated sections [31] and high storage racks composed of these [32].

Particularly noteworthy are the tests carried out on complex structural elements such as truss girders. Jankowska-Sandberg and Kołodziej [5] carried out a full-scale examination of the stability of trusses made out of hollow sections while Iwicki and Krajewski [33] examined the stability of trusses on models in a 1:4 scale. The top and bottom chords of the tested truss consisted of two angles and, additionally, battens were applied in the top chord, while the diagonals were made from closed cross-sections. The above-mentioned studies concerned the stability of the top and bottom truss chords at different transverse support conditions of both chords.

In fact, few experiments concern studies of trusses made of CFS open cross-sections. Dawe, Liu, and Li [7] conducted experimental research testing thirteen full-scale triangular truss specimens made of cold-formed C-section with edge stiffeners. Connections in the joints were made using self-drilling screws. Additionally, gusset plates were used in the supporting and ridge joints. Specimens were fabricated in three pitches: 4:12, 6:12, and 8:12. The aim of the experiments was to investigate the impact of the top chord inclination and the effectiveness of various methods of strengthening the heel connection on the increase in the load capacity of the truss. Analysis of the top chord inclination showed that an increase in truss pitch resulted in an increase in the load capacity of truss specimens. For comparative purposes, DSM (Direct Strength Method) analysis was also performed and calculations were carried out using the recommendations of Canadian standards CSA.

Dizdar, Baran and Topkaya [34] conducted experimental and numerical tests on 17 full-scale floor trusses made of cold formed sigma-type cross-sections with edge stiffeners. Diagonals were attached to chords by making use of rivets or self-tapping screws. Both the rigidity and bearing load capacity of the trusses were tested depending on such parameters as the wall thickness of the section, the number of connection fasteners used in the joint, and the method of connecting the diagonals with the chords.

Reda et al. [35] performed experimental tests on 12 triangular roof trusses made of CFS C-sections. Experimental studies allowed for a numerical model to show the actual behavior of the structure. The aim of the study was to investigate the overall behavior of CFS trusses using finite element analysis to predict the location of the truss failure and its cause by calculating the demand to capacity (D/C) ratio using the Direct Strength Method (DSM) for each component of the truss and comparing this with the results of FE analysis. The presented procedure for calculating the D/C ratio can contribute to simplifying the engineering design process by omitting the time-consuming FEM analysis.

In turn, Song et al. [36] performed tests on 5 trusses made of CFS sections joined by means of a self-piercing riveted (SPR) connection. The trusses were subjected to point bending. The influence of the trusses' height and span on their flexural stiffness and ultimate bearing capacity was investigated. As a result of parametric analyses, a theoretical formula was proposed to calculate the equivalent flexural stiffness of the trusses with SPR connections. As the formula agreed with the experiment's results, it was concluded that the proposed theoretical formula is valid and can be applied to practical engineering. Not only was the flexural stiffness and load capacity the subject of the carried out research but also lateral buckling of chords. Konkong et al. [37] studied the lateral buckling of a CFS cantilever truss. The object of their interest was expressions for the buckling length factor which are presented in AISI [38] and the Eurocode 3 [17] specification. Good conformity between experimental and analytical results was stated. It had been shown that the values of the K-factor by AISI and Eurocode 3 were too conservative for compression truss.

Zaharia and Dubina presented comprehensive studies on the rigidity of bolted joints in truss joints made of CFS members in [39]. Experimental studies carried out over several years were aimed at assessing the actual behavior of screw joints in trusses made of CFS sections. Based on tests performed on single joints and on truss fragments, a theoretical model of joint stiffness was proposed. The joint rigidity formula, which determines the buckling length of the lattice members, was also checked by testing on a full-scale structure.

Much more experimental research on the joints and connections of the CFS truss members was undertaken. Lim and Nethercot [40] investigated the stiffness of the shear connection in the ridge joint of a portal frame made of CFS channel sections. The results of experimental studies were compared with the results of the numerical analysis. The dependence of the connection stiffness on the number of bolts and the bolt spacing in the connection was proved. These studies were continued by Lim et al. [41]. Dubina [42] described the full-scale tests of lap joints in portal frame joints made of CFS channel sections.

Mathieson et al. [43,44] presented an innovative pin-joint connector called Howick Rivet Connector (HRC). The research program began with experimental tests on T-joints. Then, HRC connectors were proposed for the pinned joints in the trusses made of CFS sections. Tests were carried out on a number of trusses made of chanel-section under static and cyclic loading. Test results indicated that due to the shape of connectors considered, they can have a positive effect on the joint stiffness.

Thus, eccentricities in the joints of modern truss structures made from CFS open cross-sections are inevitable. However, the eccentricity influence on joint resistance has not been studied so far. The knowledge on sectional instability modes local or distortional buckling of individual plate elements at complex connections is still challenging and requires more effort and attention from designers as they are not entirely covered by design code procedures. Zaharina and Dubina [39] have already drawn attention to the need for such research due to the lack of standard regulations in this area.

3. Experimental investigation

The currently used methods of shaping joints by introducing diagonals inside truss chords (Fig. 1) cause that the joint area on the truss chord is stiffened by the walls of the truss members. The support conditions in the part of the hat-section web in the area of the analyzed truss chord joint are indicated in Figure 3.

Therefore, the following research hypothesis was assumed:

The resistance of truss joints made from CFS open cross-sections that are located on compression chords and have positive eccentricity is greater than the resistance that results from hitherto known methods of steel structure dimensioning. The increase in resistance in the joint originates from the local support conditions of the plane elements of the hat-section chord in the area of the truss joint.

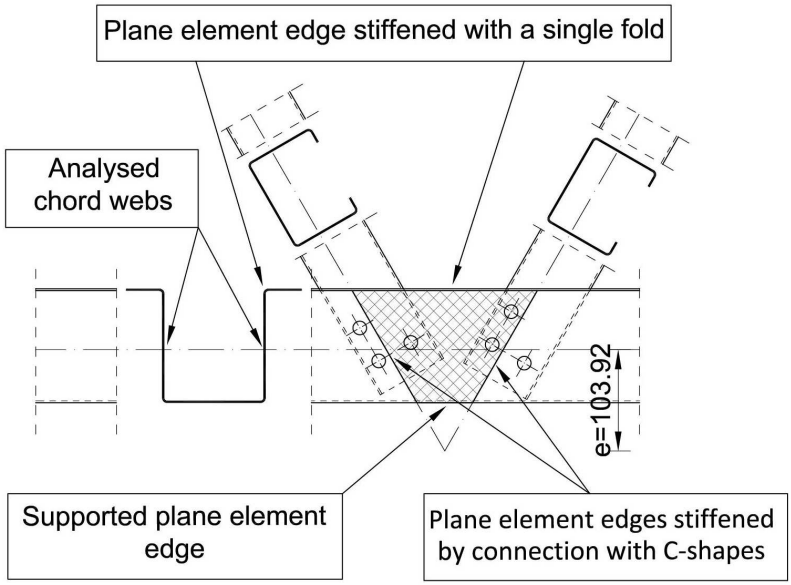

Fig.3. Support conditions of the hat-shaped section plane element in the area of the truss joint.

In order to prove the above hypothesis, experimental studies of a typical joint used by one of the well-known companies involved in the design and manufacturing of steel structures from CFS sections were undertaken at Gdańsk University of Technology. Due to the high cost of such studies, the experiment was carried out only for one wall thickness of sections, and the obtained results allowed the development of a correct numerical model.

3.1. Experiment arrangement

3.1.1. Research model

Experimental studies were carried out in a laboratory of Gdańsk University of Technology, Poland. A full-scale research model of the truss fragment made of CFS open cross-sections was designed. The geometry of the truss adopted for testing is shown in

Figure 4a. Chords were made from the hat-section H 39/117/106/117/39x2, while diagonals were made from the channel-section C 17/75/100/75/17x2 (Fig. 4b, c). Due to the shape of the cross-sections used for the lattice member profiles (open cross-sections), the diagonals were inserted into introduced inside the chords, as was done in [15], and [6]. With such a method of joint shaping, screw connectors are most often used. In the investigated truss segment, 6 bolts M12, class 8.8 were used in each joint (3 bolts on each web), as shown in Figure 4a).

The joint with the value of the eccentricity e = 103.92 mm located on the compression chord was tested, as only walls of compressed members are subjected to the local loss of stability.

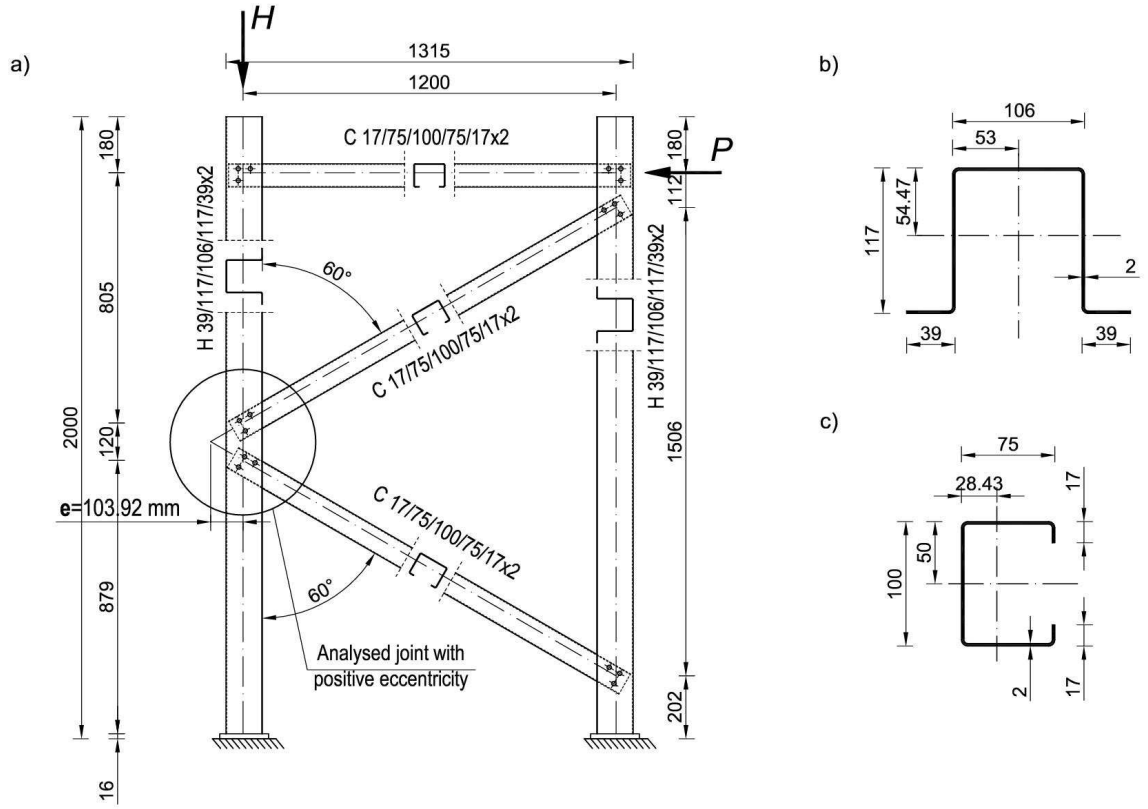

Fig. 4. a) research model; static scheme, dimensions of sections used in experimental tests for: b) chords, c) diagonals. (All dimensions in mm)

3.1.2. Research stage

The static scheme of the research model is shown in Figure 4. The model was loaded with two point forces H and P. Force H causes compression of the bottom chord, while force

P causes, due to the natural distribution of internal forces in the eccentric joint, local shearing/bending of the bottom chord in the area of the joint. The use of a stationary actuator to introduce force H (Fig. 5a) would change the static scheme of the cantilever mounted tested model by immobilizing the free end of the truss in joint C. Therefore, a special compression head was applied to introduce force H via two turnbuckles. This allowed for the free displacement of joint C under the action of force P (Fig. 5b).

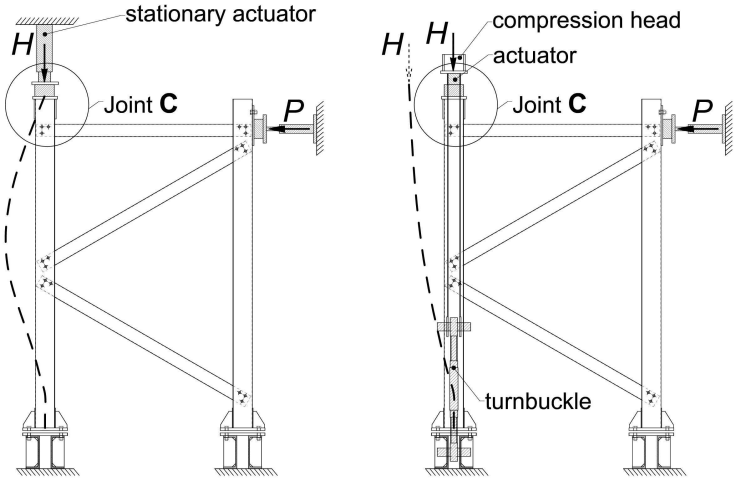

Fig. 5. Research model scheme of work when using: a) stationary actuator, b) compression head [8].

One of the tested models fixed on the research station is shown in Figure 6. The stand was developed after a series of preliminary numerical analyses and after the preliminary tests described in [8,19]. The support and auxiliary elements of the experimental station were painted yellow.

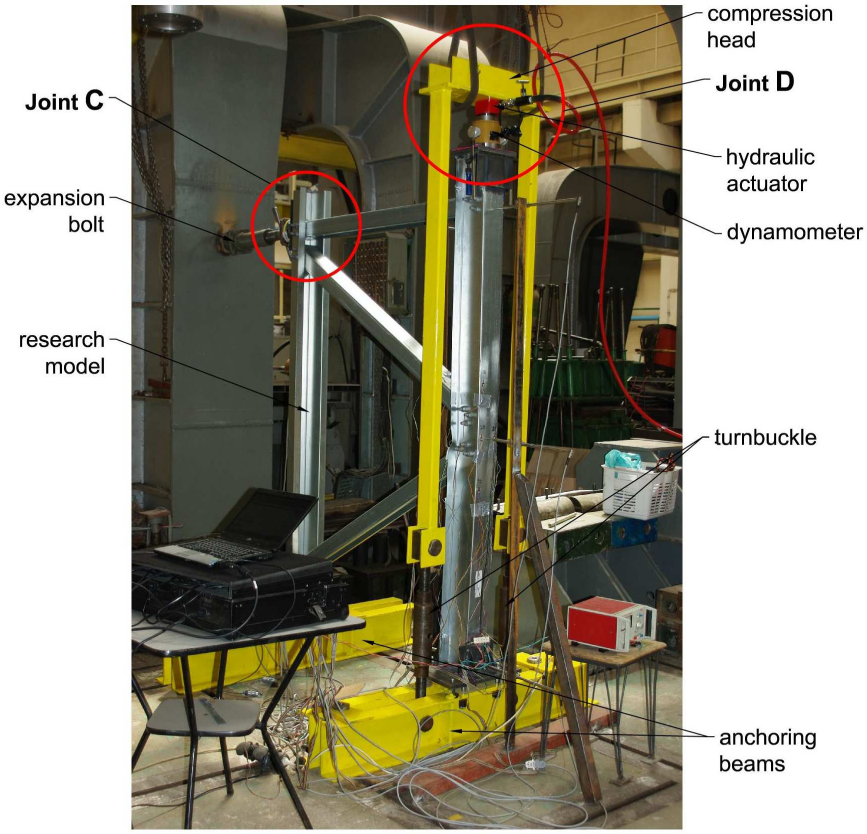

Fig. 6. Truss segment on the research station.

3.1.3. Applied instruments

The following measuring equipment was used during the tests. Seven inductive displacement sensors with a measuring range of ±100 mm were applied and arranged on the structure according to the diagram in Figure 7. The inductive sensors X and Y measured displacements of the research model in the bending plane, and sensor Z measured displacements out of the bending plane. Displacement sensors W1, W2, T1, and T2 were used to control possible horizontal and vertical displacements of support joints. For strain measurements, linear electrical resistance strain gauges LY11-6 / 120A were applied in four measuring cross-sections. The three cross-sections were placed on the compression chord (hat-section), respectively: 1-1 above the examined joint, 2-2 on the axis of the joint and 3-3 below the joint, and one additional cross-section 4-4 on the compression diagonal. The layout of the strain gauges in each of the cross-sections is shown in Figure 7. In total, 16 strain gauges were used, including one compensating strain gauge. Four strain gauges were

applied at every cross-section. Symmetrical about both local axes (z-z and y-y) strain gauges layout assured monitoring of the strains and type of stresses. The same values of the readings of the strain gauges A, B, C, and D indicated axial compression. In the case of bending about axis y-y, the readings were expected to be the same but only on two strain gauges at each side of the bending axis (A=C and B=D). When bending about axis z-z the equal readings were on the opposite sides of the bending axis (A=B and C=D).

During the tests, two point forces P and H were applied to the structure respectively by means of the expansion bolt and the actuator BVA HF2005 with a lifting capacity of 20 tons. The value of force P was registered using a dynamometer, N.B.C. Elettronica, with a nominal range of ±100 kN located between the expansion bolt that was causing force P and the tensioned chord of the structure, whereas the value of force H was measured by a CZAH CT 25 dynamometer with a rated load of 250 kN, located below the compression head and at the top of the compression chord of the research model.

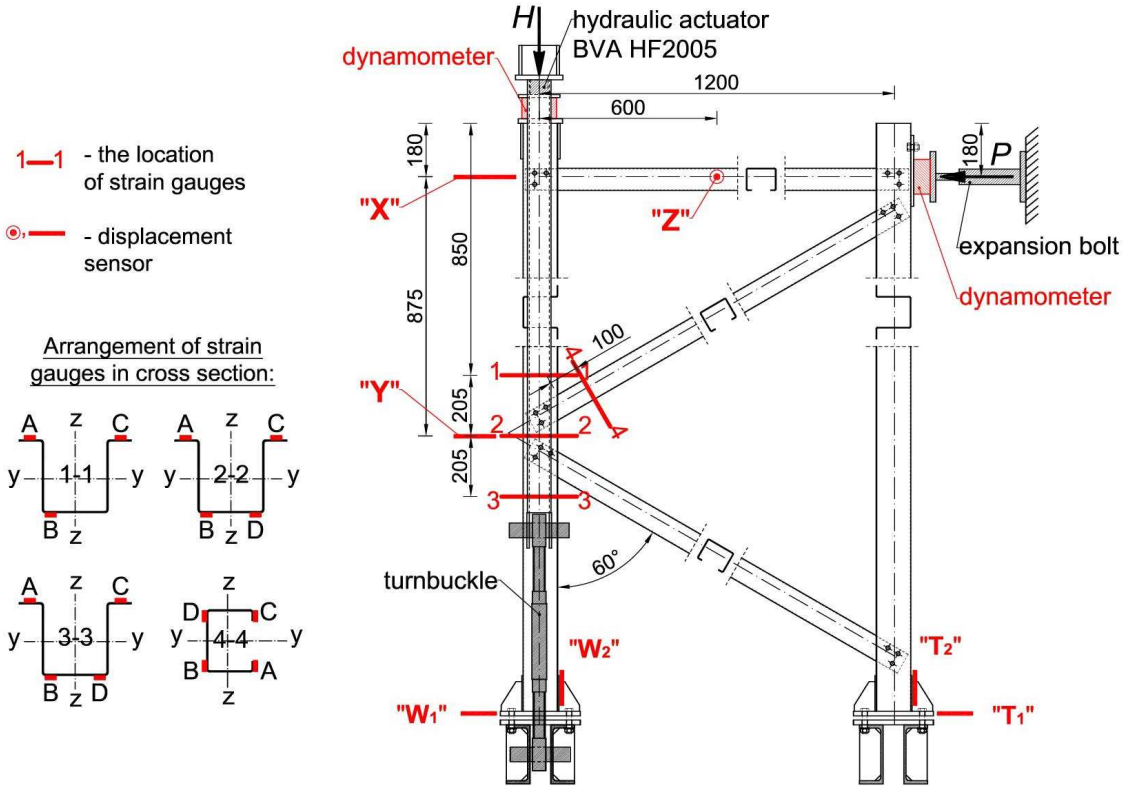

Fig. 7. Schematic layout of the measuring equipment on the research model.

3.2. The course and results of experimental studies

3.2.1. The course of experimental research

Five research models with subsequent numbers 1, 2, 3, 4 and 5 were subjected to testing. Procedures for preparing and conducting the described tests were carried out in accordance with the standard EN 1993-1-3 [17]. The destructive tests of the models were preceded by uniaxial tensile tests, which were the basis for identification of material constants and determination of the relation σ-ε of the steel material from which the members of research models were made. The tests were executed on samples cut from sections used for truss models build. 18 samples were gained from the hat section and 12 samples from the channel-section. Based on the obtained test results, the following average values of material properties were determined:

- hat-section E=210 GPa, f_y=398 MPa, f_u=489 MPa,
- channel-section E=199 GPa, f_y=366 MPa, f_u=445 MPa.

Load application to research models with turnbuckles was preceded by control and equalization of the tension force values in the tensioning elements of the compression head. Application of load to the structure was carried out at two stages:

- Stage I - applying force H,
- Stage II - applying force P.

The forces were put on the structure by gradually increasing their value. Force H (compression) was introduced in 10 kN increments until the value of 100 kN was reached. From that moment, the value of force H was not changed as its task was only to achieve a certain level of normal stress in the analyzed cross-section. Next, the second stage of loading proceeded, i.e. the introduction of force P, with a step of 5 kN. There was a local loss of stability of member walls in the area of the analyzed joint (Fig. 11a) in all five models, already within the range of force P values from 5 kN to 10 kN. However, the bending load P was still increased up to a value of about 40 kN in order to determine the mechanisms of

destruction of the bending joint area (Fig. 11b). The course of introduced loads at time “t” recorded during destructive tests is shown in Figure 8 as illustrated in the results obtained during the testing of model No. 4. It should be noted that the time course of the load was analogous in all five models.

Based on the analysis of the course of the introduced load, it can be seen that an increase in the value of force P causes a simultaneous decrease in the value of force H (Fig. 8). It should be pointed out that after starting the introduction of load P, it was not possible to maintain the value of force H at a constant level due to the instrumentation used. At the same time, it should be noted that this fact was not significant due to the purpose of the study, which was to lead to a possible destruction of the compression chord under the influence of bending moment load in the area of the analyzed joint. However, the values of both forces were accurately recorded (Fig. 8).

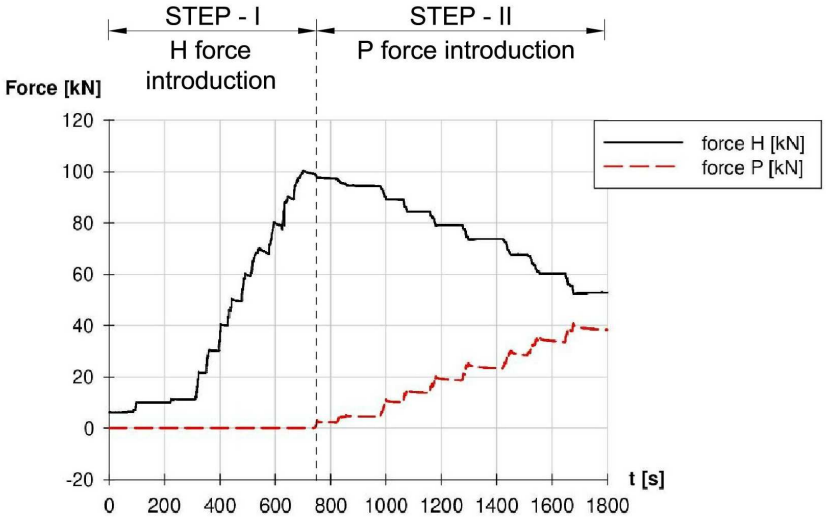

Fig. 8. Load history in time “t” registered during tests, as illustrated in based on the example of model No. 4.

3.2.2. Results of research

Due to the purpose of the study, which was to determine the forms of deformation of the hat-section walls and strains near the analyzed joint while applying the load, the strain values were registered with strain gauges in four measuring cross-sections (Fig. 7). The

courses of strains as a function of time, specified in all four measurement cross-sections and registered during tests on model No. 4 are shown in Fig.9.

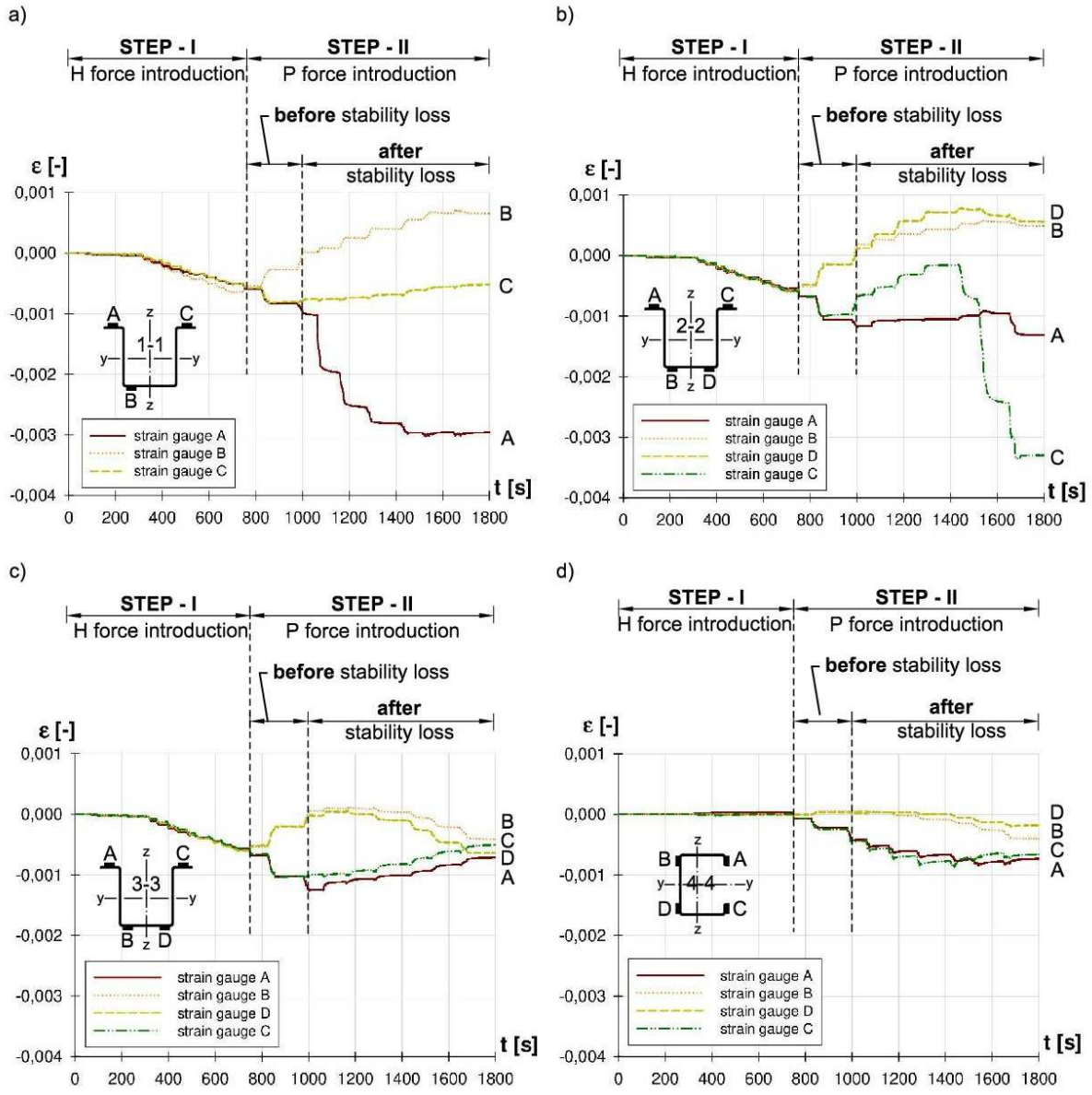

Fig. 9. The course of strains as a function of time in cross-sections: a) 1-1, b) 2-2, c) 3-3, d) 4-4, as illustrated in model No. 4 (description in the text).

Based on the charts presented in Figure 9, it was observed that at the first stage of the loading, i.e. while introducing force H, there is compliance between the readings of the strain gauges A, B, C and D in all four measuring cross-sections, which indicates an even distribution of stress in the compressed cross-section. In addition, it should be pointed out that at the first stage of loading no forms of deformations of the research model members

were observed. During the second stage of loading, in the range before local loss of stability, symmetrical increases (A, C strain gauges) or reductions (B, D strain gauges) of cross-sectional strains were observed relative to the local y-y axis ("clean" bending). Nevertheless, in the range after the loss of stability, it was observed that the deformation shape loses its symmetrical form. The cantilever walls of the hat-sections were characterized by different directions of strains (measured with A and C strain gauges). The lack of symmetry relative to the local z-z axis during deformation is caused by the existence of various imperfections.

Forms of truss chord stability loss under compression and bending identified on the basis of the destructive tests of five research models are presented in Figure 10. The loss of stability always started in the measuring cross-section 2-2 and, as the load increased, deformations increased gradually. In all examined cases only a local form of loss of stability occurred, what is visible in Figures 10, 11a and 11b. Typical plastic mechanism of failure when columns build from open cross-sections are subjected to eccentric compression [45,46] had been observed. It was CF1 when the flange is an outstanding compression element and CW1 when the web of the cross-section is an internal compression element (flip disc type).

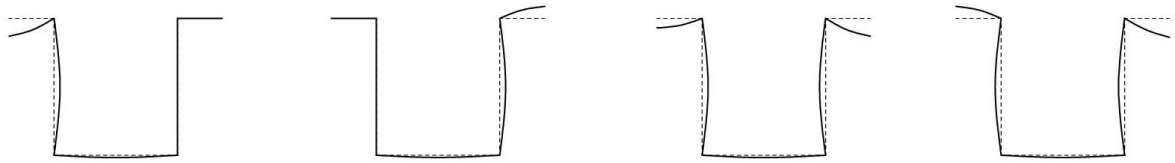

Fig. 10. Forms of truss chord local stability loss.

Deformation forms of the hat-section walls in the area of the analyzed joint at the beginning of the stability loss are presented in Figure 11a, while Figure 11b presents the deformation form of the hat-section observed during the experiment for the final stage of loading (P=40 kN, H_{cor}=55 kN).

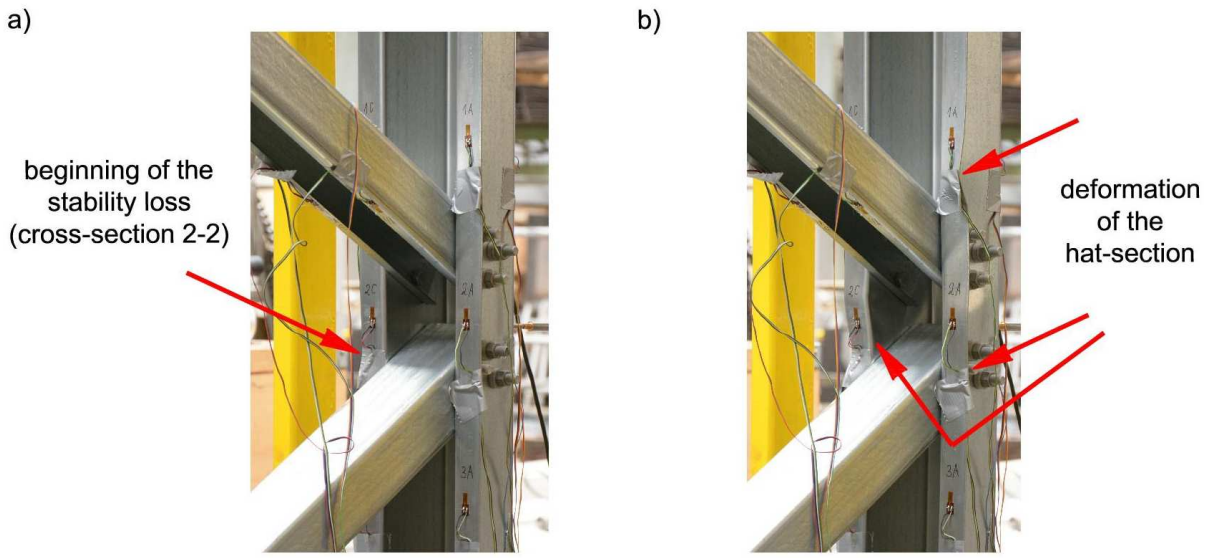

296

297 **Fig. 11.** a) beginning of the hat-section stability loss for the load value P=5 kN, H_{cor}=95 kN,
298 b) deformation of the hat-section chord at the final stage of the load.

299 The values of the external load of the research model as a set of forces, P and the
300 corresponding force H, are summarized in Table 1. These are the values at which the
301 beginning of the loss of local stability of the member walls in the vicinity of the analyzed joint
302 was observed. It was also observed that in all the research models in cross-section 2-2 or
303 directly in its vicinity, permanent deformations of the hat-section corners occurred. This
304 indicates that the material yield point was reached in this section area (Fig. 12). The yielding
305 state of the corners in the area of the analyzed joint was considered the limit state of the load
306 capacity of the analyzed cross-section.

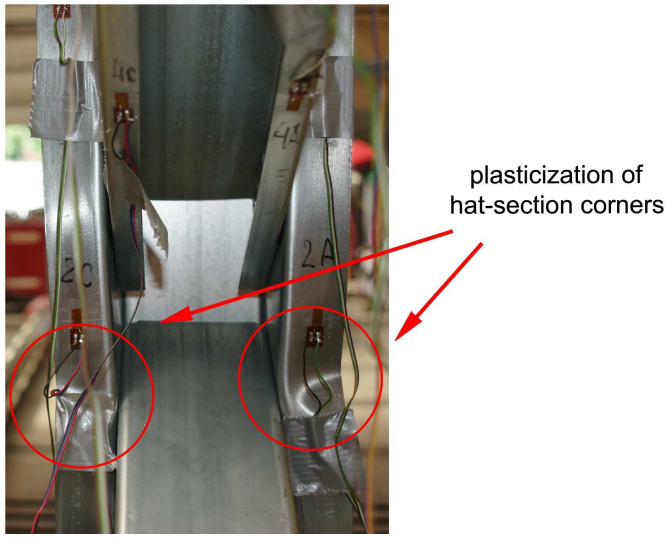

307

Fig. 12. Yielding of the hat-section corners in the measuring cross-section 2-2 (based on the example of research model no. 2).

Considering the above, the beginning of the stability loss observed during the tests can be qualified as the attainment of the critical state of the cross-section, and the load values given in Table 1 as the critical load of the research model (in the form of a set of P and H forces). When the above-mentioned load was reached, it was considered that the structure was working in a supercritical state until it reached the limit state. The observed variation of the forces P and H_{cor} is resulting from the "eye method" applied for identification of the stability loss moment during the conducted experiments. Received values of the forces were verificated with the use of elaborated diagrams presented in Figure 9. The variation of force P ranging from 5 to 8,5 KN is acceptable when statistical analysis is done. The test results presented in Table 1 showed good convergence of results for all models. All results are within +/- 2 standard deviations, which indicates good repeatability of the experiment.

Table 1. Listing of corresponding values of P and H_{cor} forces at which the local stability loss of the compressed chord of the truss model occurred.

Research model number	**Force** **P [kN]**	**Average value of force P** P_{av} **[kN]**	**Standard deviation** s_P **[-]**	**Corresponding force H** H_{cor} **[kN]**	**Average value of force H** $H_{cor,av}$ **[kN]**	**Standard deviation** s_H **[-]**
Model **1**	5.0	6.58	1.58	106	94.6	7.43
Model **2**	8.5			96		
Model **3**	7.7			89		
Model **4**	5.0			95		
Model **5**	6.7			87		

After carrying out destructive tests, the models were unscrewed to check for damage to fasteners and holes. It is visible in Figure 13 that there was no damage to the holes in the walls of the hat or channel-shaped sections. Bolts M12 class 8.8 used in the connection were also not damaged.

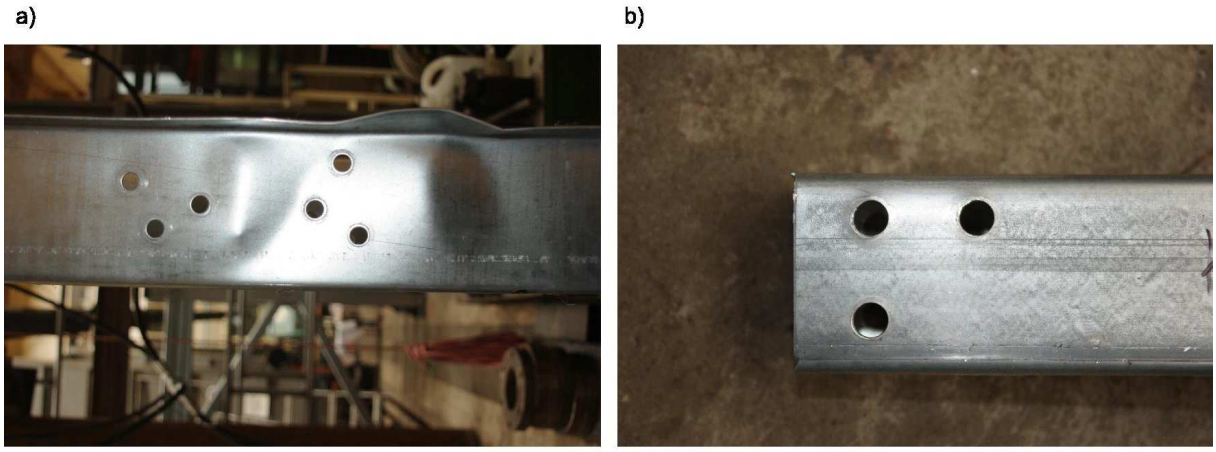

Fig. 13. View of bolt holes in deformed truss members during the experiment: a) hat-section, b) channel-section.

Model displacements at X, Y and Z measurement points are shown in Figure 14. The lateral displacement values (in the plane perpendicular to the plane of the truss) resulting from the "Z" sensor and which ranged from -2.28 mm to 4.65 mm, were considered insignificant. In turn, the control of model support displacements showed minimal rotation and support displacement.

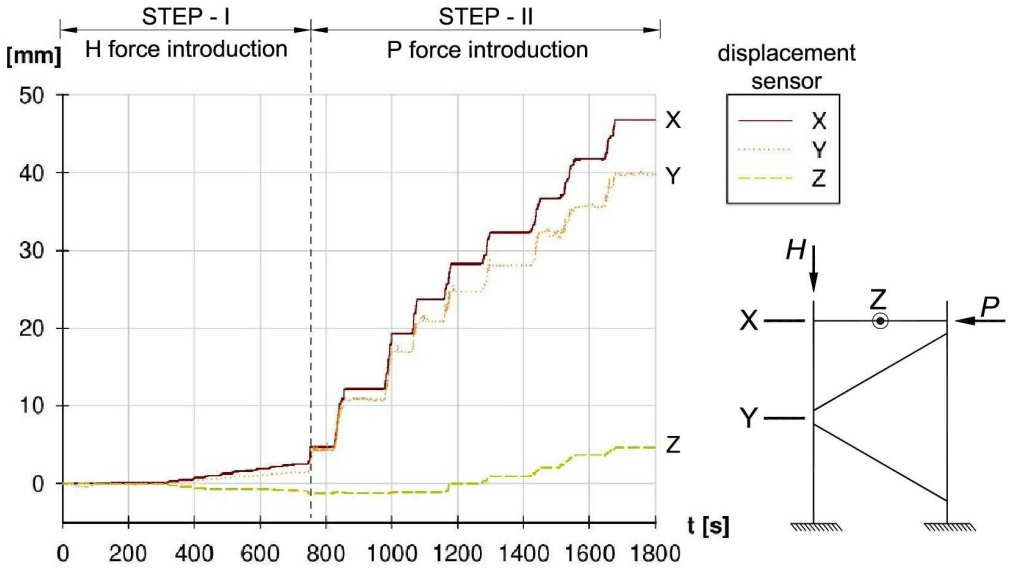

Fig. 14. Model displacements at X, Y, Z measurement points – illustrated in model No. 4.

4. Eurocode 3 design procedure.

For comparative purposes, the stress intensity of cross-sections 1-1, 2-2 and 3-3 in the research truss joint was checked using analytical design procedures covered by European standards [14,16–18].

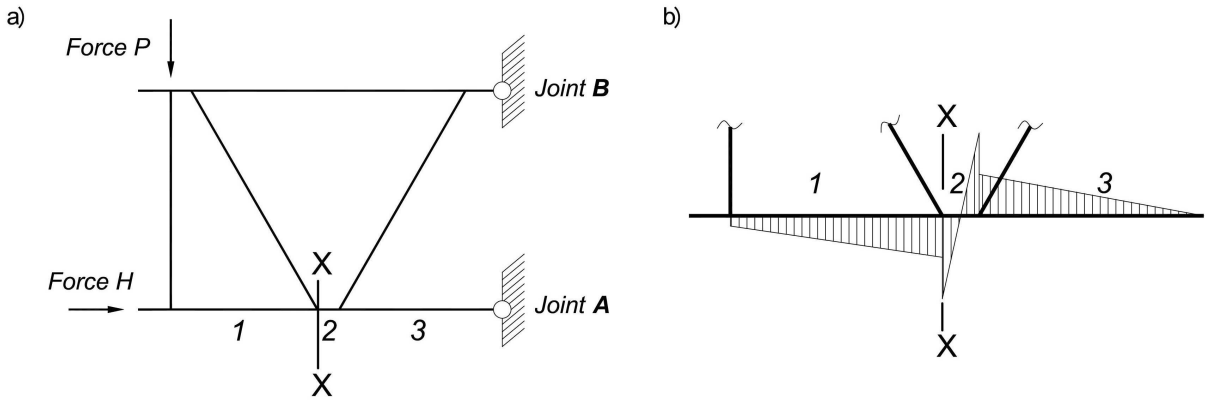

Fig. 15. a) Static scheme of the analyzed truss with the numbering of the compression chord members, b) bending moment diagram at the compression truss chord.

In the analyzed case (Fig. 15), in the cross-section X-X (no 2), due to the positive eccentricity that occurs, in addition to normal forces shear forces and bending moments also occur. Taking into account the forces in member No 2 and in members No 1 and 3, respectively, the effort of the cross-section was calculated on the basis of the standard formula (1) [17]. The analysis was carried out in the elastic range. The calculations were performed for an eccentricity with value e = 103.92 mm and sections with a wall thickness of 2 mm. The value of the eccentricity e = 103.92 mm results from the geometry of the truss (angle of inclination of the diagonals), dimensions of the connected members, and the connectors used.

$$N_{Ed}/N_{c,Rd}+(M_{y,Ed}+\Delta_{My,Ed})/M_{cy,Rd,com} \quad (1)$$

where:

N_{Ed} – design value of the compression force,

$M_{y,Ed}$ – design value of the bending moment (resulting from the eccentricity at the joint),

$\Delta M_{y,Ed}$ – additional bending moment (due to a shift of the centroidal axis of the effective cross-section relative to the centroidal axis of the gross cross-section (for class 4),

$N_{c,Rd}$ – design resistance of a cross-section for uniform compression,

$M_{cy,Rd,com}$ – moment resistance for the maximum compressive stress in a cross-section that is subjected only to moment about y-y axis.

It should be noted that, in accordance with the Eurocode procedure, for the calculations of the degree of the cross-section effort to have value in engineering terms, the random nature of both the loads and the research model should be taken into account. Loads in experimental studies are deterministic. In order to obtain random values, 84% quantile of H and P load values corresponding to mean values of H and P force increased by one standard deviation respectively were used in calculations. Table 2 presents effort values in three analysed cross-sections for four selected load cases (set of forces H and P).

Table 2. Effort of cross-sections of truss members Nos. 1, 2, 3 (according to Fig. 15)

e=103.92 mm					
quantiles of forces		Member no. / cross-section	Internal forces		Effort of the compression and bending cross-section [%]
H [kN]	P [kN]		N_{Ed} [kN]	M_{Ed} [kNm]	2.0 mm
108	0	1 (1-1)	107.79	0.13	70.58
		2 (2-2)	107.96	0	69.02
		3 (3-3)	108	0	69.05
102	6	1 (1-1)	101.94	0.38	70.05
		2 (2-2)	106.55	0.55	75.19
		3 (3-3)	111.10	0	71.03
85	23	1 (1-1)	85.35	1.24	70.50
		2 (2-2)	102.32	1.78	88.29
		3 (3-3)	119.88	0.39	81.65
57	47	1 (1-1)	57.95	2.56	69.94
		2 (2-2)	92.46	3.64	105.88
		3 (3-3)	128.28	0.77	91.91

When force P is equal zero, there is only axial compression and the effort of every one cross-section was comparable. Introduction even a small value of the force P caused cross-section bending due to the eccentric loading of the joint. This led to an increase in effort in the measuring cross-section 2-2 in member 2 in comparison with the cross-sections 1-1 and 3-3 located on members 1 and 3. In summary, the introduction of force P resulted in the following: The effort of the cross-section in member No. 2 (in the joint) is always greater than the effort of the cross-section in members Nos. 1 and 3, which of course is associated with the occurrence of shear forces and bending moments (a consequence of positive eccentricity). At the final stage of the research model loading we are dealing with a special case when the nodal cross-section is overloaded (as was confirmed by experimental tests) while maintaining the resistance condition outside the joint. Therefore, it is logical that in a design situation, exceeding the load capacity in the joint is already a signal for the designer to increase the cross-section of the entire truss chord or make reinforcing cover plates (Fig. 2). So, according to the Eurocode procedure, the cross-sectional load capacity of the eccentric joint is decisive when the truss chord cross-section is selected.

5. Summary and conclusions

The conducted experimental tests were aimed at obtaining information on the behaviour of trusses made of CFS with positive eccentricity at joints, as well as obtaining the research results in the form of a register of strains and displacements of both the model and the joint. The calculations of the analyzed truss segment carried out in accordance with Eurocode procedures coincide with the results of experimental tests for a truss made of 2 mm thick sections. Based on the experimental research the following conclusions were made:

- Local buckling of the hat-section chord was observed.
- The loss of stability in all research models started in the middle of the joint, in the vicinity of the measuring cross-section 2-2.

- Plastic mechanisms of failure occurred only in truss members.
- Neither bolts nor holes for fasteners were destroyed.

Due to the high cost of experimental research, destructive tests were limitated to one wall thickness, so it was not possible to explicitly confirm the research hypothesis formulated at this stage of work. In order to be able to answer the hypothesis, numerical analyses are planned for the wall thicknesses: 1.0 mm, 1.5 mm, and 4.0 mm and for different eccentric values. What is more the results of experimental tests will constitute the basis for validation of the numerical models.

6. References

[1] P. Deniziak, K. Winkelmann, TS-based RSM-aided design of cold-formed steel stiffened C-sectional columns susceptible to buckling, Shell Struct. Theory Apl. (2018) 533–536.

[2] A. Crisan, V. Ungureanu, D. Dubina, Behaviour of cold-formed steel perforated sections in compression: Part 2—numerical investigations and design considerations, Thin-Walled Struct. 61 (2012) 97–105. https://doi.org/10.1016/j.tws.2012.07.013.

[3] D. Dubina, V. Ungureanu, Behaviour of multi-span cold-formed Z-purlins with bolted lapped connections, Thin-Walled Struct. 48 (2010) 866–871. https://doi.org/10.1016/j.tws.2010.04.003.

[4] P. Paczos, K. Magnucki, Local buckiling of cold-formed thin-walled cannel beams with drop flange, Adv. Trends Struct. Mech. Comput. - Zingoni Ed. (2010).

[5] J. Jankowska-Sandberg, J. Kołodziej, Experimental study of steel truss lateral–torsional buckling, Eng. Struct. 46 (2013) 165–172. https://doi.org/10.1016/j.engstruct.2012.07.033.

[6] D. Visy, S. Adany, A.L. Joo, Finite element studies on the global buckling of cold-formed trusses., Eighth Int. Conf. Adv. Steel Struct. (2015) 1–18.

[7] J.L. Dawe, Y. Liu, J.Y. Li, Strength and behaviour of cold-formed steel offset trusses, J. Constr. Steel Res. 66 (2010) 556–565. https://doi.org/10.1016/j.jcsr.2009.10.015.

[8] M. Gordziej-Zagórowska, E. Urbańska-Galewska, P. Deniziak, Ł. Pyrzowski, Truss joint with positive eccentricities – experimental research, Civ. Environ. Eng. Rep. (2017) 107–123.

[9] J. Bródka, M. Broniewicz, Konstrukcje stalowe z rur, Arkady, Warszawa, 2001.

[10] J. Bródka, M. Broniewicz, Konstrukcje stalowe z kształtowników zamkniętych, Polskie Wydawnictwo Techniczne, Rzeszów, 2016.

[11] J.A. Packer, J. Wardenier, Y. Kurobane, D. Dutta, N. Yeomans, Design guide for rectangular hollow (RHS) joints under predominantly static loading., CIDECT Construction with hollow stell sections, Koln, 1992.

[12] J. Wardenier, Y. Kurobane, J.A. Packer, D. Dutta, N. Yeomans, Design guide for circular hollow section (CHS) joints under predominantly static loading., CIDECT Construction with hollow stell sections, Koln, 1991.

[13] Y. Chen, J. Yang, K. Hu, Parametric study and formulae of SCFs for positive large eccentricity CHS N-joints, J. Constr. Steel Res. 120 (2016) 117–131. https://doi.org/10.1016/j.jcsr.2016.01.005.

[14] EN 1993-1-8, Eurocode 3: Design of steel structures - Part 1-8: Design of joints, Eur. Comm. Stand. (2005).

[15] C. Basaglia, D. Camotim, GBT-based buckling analysis of cold-formed steel trusses, Proc. Sixth Int. Conf. Thin Walled Struct. Timisoara Rom. (2011) 149–156.

[16] EN 1993-1-1, Eurocode 3: Design of steel structures - Part 1-1: General rules and rules for buildings, Eur. Comm. Stand. (2005).

[17] EN 1993-1-3, Eurocode 3: Design of steel structures - Part 1-3: General rules - Supplementary rules for cold-formed members and sheeting, Eur. Comm. Stand. (2006).

[18] EN 1993-1-5, Eurocode 3: Design of steel structures - Part 1-5: General rules - Plated structural elements, Eur. Comm. Stand. (2006).

[19] M. Gordziej-Zagórowska, E. Urbańska-Galewska, Ł. Pyrzowski, P. Deniziak, A. Łukowicz, Preliminary experimental research on stability of truss joint with positive

452 eccentricity., Recent Prog. Steel Compos. Struct. Proc. 13th Int. Conf. Met. Struct. Zielona
453 Góra Pol. (2016) 425–432.
454 [20] J. Ye, S.M. Mojtabaei, I. Hajirasouliha, Local-flexural interactive buckling of standard
455 and optimised cold-formed steel columns, J. Constr. Steel Res. 144 (2018) 106–118.
456 https://doi.org/10.1016/j.jcsr.2018.01.012.
457 [21] J. Ye, I. Hajirasouliha, J. Becque, Experimental investigation of local-flexural
458 interactive buckling of cold-formed steel channel columns, Thin-Walled Struct. 125 (2018)
459 245–258. https://doi.org/10.1016/j.tws.2018.01.020.
460 [22] A. Łukowicz, E. Urbańska-Galewska, Deformations of innovative cold-formed GEB
461 section., 7th Eur. Conf. Steel Compos. Struct. EUROSTEEL. (2014) 1–6.
462 [23] M.S.H.M. Sani, F. Muftah, C.S. Tan, Experimental Analysis of Cold-Formed Steel C-
463 Sections with the Notch Subjected to Axial Compression, KSCE J. Civ. Eng. 24 (2020) 1228–
464 1239. https://doi.org/10.1007/s12205-020-2340-z.
465 [24] M.R. Haidarali, D.A. Nethercot, Finite element modelling of cold-formed steel beams
466 under local buckling or combined local/distortional buckling, Thin-Walled Struct. 49 (2011)
467 1554–1562. https://doi.org/10.1016/j.tws.2011.08.003.
468 [25] D. Dubina, V. Ungureanu, L. Gîlia, Experimental investigations of cold-formed steel
469 beams of corrugated web and built-up section for flanges, Thin-Walled Struct. 90 (2015)
470 159–170. https://doi.org/10.1016/j.tws.2015.01.018.
471 [26] M. Kotełko, Load-capacity estimation and collapse analysis of thin-walled beams and
472 columns—recent advances, Thin-Walled Struct. 42 (2004) 153–175.
473 https://doi.org/10.1016/S0263-8231(03)00055-7.
474 [27] C. Yu, B.W. Schafer, Simulation of cold-formed steel beams in local and distortional
475 buckling with applications to the direct strength method, J. Constr. Steel Res. 63 (2007) 581–
476 590. https://doi.org/10.1016/j.jcsr.2006.07.008.
477 [28] A. Łukowicz, E. Urbańska-Galewska, M. Gordziej-Zagórowska, Experimental testing
478 of innovative cold-formed GEB section., Civ. Environ. Eng. Rep. (2015) 129–140.

[29] C.H. Pham, G.J. Hancock, Tension field action for cold-formed sections in shear, J. Constr. Steel Res. 72 (2012) 168–178. https://doi.org/10.1016/j.jcsr.2011.12.001.

[30] C.H. Pham, G.J. Hancock, Numerical investigation of longitudinally stiffened web channels predominantly in shear, Thin-Walled Struct. 86 (2015) 47–55. https://doi.org/10.1016/j.tws.2014.09.005.

[31] A. Crisan, V. Ungureanu, D. Dubina, Behaviour of cold-formed steel perforated sections in compression. Part 1—Experimental investigations, Thin-Walled Struct. 61 (2012) 86–96. https://doi.org/10.1016/j.tws.2012.07.016.

[32] A. Crisan, V. Ungureanu, D. Dubina, Influence of web members on the in-plane and out-of-plane capacities of steel storage upright frames, Thin-Walled Struct. 81 (2014) 175–184. https://doi.org/10.1016/j.tws.2013.10.024.

[33] M. Krajewski, P. Iwicki, Stability and laod bearing capacity of a braced truss under upward wind loading, Eurosteel. (2017).

[34] C. Dizdar, E. Baran, C. Topkaya, Strength and stiffness of floor trusses fabricated from cold-formed steel lipped channels, Eng. Struct. 181 (2019) 437–457. https://doi.org/10.1016/j.engstruct.2018.12.041.

[35] M. Reda, T. Sharaf, A. ElSabbagh, M. ElGhandour, Behavior and design for component and system of cold-formed steel roof trusses, Thin-Walled Struct. 135 (2019) 21–32. https://doi.org/10.1016/j.tws.2018.10.038.

[36] L. Song, W. Yan, C. Yu, Z. Xie, Q. Tan, Flexural behavior investigation of the CFS truss beams with self-piercing riveted connection, J. Constr. Steel Res. 156 (2019) 28–45. https://doi.org/10.1016/j.jcsr.2019.01.014.

[37] N. Konkong, T. Aramraks, K. Phuvoravan, Buckling length analysis for compression chord in cold-formed steel cantilever truss, Int. J. Steel Struct. 17 (2017) 775–787. https://doi.org/10.1007/s13296-017-6031-7.

[38] AISI, North American specification for the design of cold-formed steel structural members., Am. Iron Steel Inst. (2012).

[39] R. Zaharia, D. Dubina, Stiffness of joints in bolted connected cold-formed steel trusses, J. Constr. Steel Res. 62 (2006) 240–249. https://doi.org/10.1016/j.jcsr.2005.07.002.

[40] J.B.P. Lim, D.A. Nethercot, Stiffness prediction for bolted moment-connections between cold-formed steel members, J. Constr. Steel Res. 60 (2004) 85–107. https://doi.org/10.1016/S0143-974X(03)00105-6.

[41] J.B.P. Lim, G.J. Hancock, G. Charles Clifton, C.H. Pham, R. Das, DSM for ultimate strength of bolted moment-connections between cold-formed steel channel members, J. Constr. Steel Res. 117 (2016) 196–203. https://doi.org/10.1016/j.jcsr.2015.10.005.

[42] D. Dubina, Structural analysis and design assisted by testing of cold-formed steel structures, Thin-Walled Struct. 46 (2008) 741–764. https://doi.org/10.1016/j.tws.2008.01.030.

[43] C. Mathieson, K. Roy, G.C. Clifton, A. Ahmadi, J.B.P. Lim, Failure mechanism and bearing capacity of cold-formed steel trusses with HRC connectors, Eng. Struct. 201 (2019) 109741. https://doi.org/10.1016/j.engstruct.2019.109741.

[44] C. Mathieson, K. Roy, G.C. Clifton, A. Ahmadi, M. Rehan, J.B.P. Lim, Novel pin jointed moment connection for cold-formed steel trusses, Steel Compos. Struct. (2019) 453–467.

[45] V. Ungureanu, M. Kotełko, J. Grudziecki, Plastic mechanisms for thin-walled cold-formed steel members in eccentric compression, (2016).

[46] M. Kotełko, Nośność i mechanizmy zniszczenia konstrukcji cienkościennych., Wydawnictwo WNT, Warszawa, 2011.